Nanoscale

Accepted Manuscript

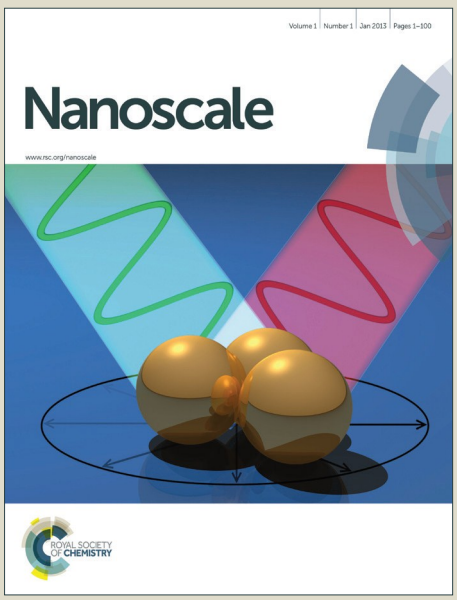

ROYAL SOCIETY OF CHEMISTRY

www.rsc.org/nanoscale

Journal Name

RSCPublishing

ARTICLE

Versatile method for AFM-tip functionalization with biomolecules: fishing a ligand by means of an *in situ* click reaction†

Rakesh Kumar,‡[a] Shivaprakash N. Ramakrishna,‡[b], Vikrant V. Naik,[b] Zonglin Chu,[a] Michael E. Drew,[a] Nicholas D. Spencer,*[b] and Yoko Yamakoshi*[a]

Cite this: DOI: 10.1039/xoxxoooooox

Received ooth January 2012,
Accepted ooth January 2012

DOI: 10.1039/xoxxoooooox

www.rsc.org/

A facile and universal method for the functionalization of an AFM tip has been developed for chemical force spectroscopy (CFS) studies of intermolecular interactions of biomolecules. A click reaction between tripod–acetylene and an azide–linker–ligand molecule was successfully carried out on the AFM tip surface and used for the CFS study of ligand–receptor interactions.

Introduction

Chemical force microscopy/spectroscopy (CFM/CFS), which utilizes chemically functionalized AFM tips, provides a useful method for studying intermolecular interactions at the single-molecule level.[1-3] Recently, this approach has received much attention for investigating various biological processes, such as protein unfolding,[4-6] ligand–receptor interactions,[7,8] antibody–antigen interactions[9,10] and interactions between DNA strands.[11-13] For single-molecule force spectroscopy (SMFS), the stable immobilization of ligands on the AFM tip is critical.[14,15] Creation of self-assembled monolayers (SAMs) of alkane thiols on the Au-coated AFM tip is the most common approach for chemical functionalization of the AFM tip.[1-3,15-17] However, using such SAM systems, CFM measurements do not always provide reproducible, accurate SMFS data and therefore, on the AFM tip, a sufficiently stable method of attachment of ligands with optimal density is required.[18] Considering these challenges and based on Keana's work,[19, 20] we previously developed a new class of molecular tripods (*e.g.* molecules **1** and **2** in Fig. 1) for the robust attachment of biomolecules onto the gold-coated AFM tip through a total of six Au–S covalent bonds.[21] In addition, a wider tripod scaffold was essential to achieve a well-controlled orientation of the ligand (far from the tip surface and close to the receptors immobilized on the substrate) and further realize a lower density of ligand on the AFM tip to enable the ideal conditions for more accurate single-molecule studies.[19-27] In the previous report, the efficiency and reliability of this tripod system was tested by a standard unbinding study of biotin and NeutrAvidin using a biotin-derived tripod **2** (Fig. 1c) in comparison to the SAM system.[21] The tripod system provided more accurate and reproducible rupture-force data compared to a control SAM experiment, and was in good agreement with previously reported values by other groups.[28]

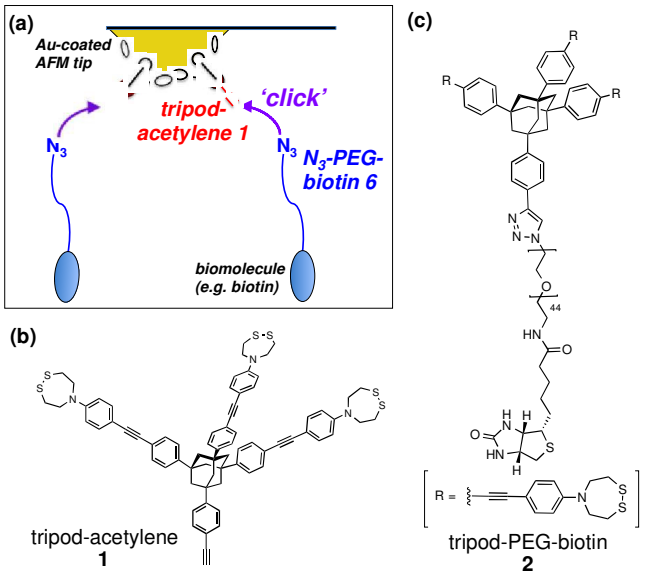

Fig. 1. (a) Schematic illustration of AFM-tip functionalization by the *in situ* click reaction of N_3–PEG–biomolecule with tripod–acetylene **1**, pre-attached onto the Au-coated AFM tip, (b) tripod–acetylene **1** used for the pre-funtionalization of AFM tip, and (c) a tripod–PEG_{2000}–biotin molecule **2** used for standard measurements.

Despite the great advantages that tripod-derived molecular tips provided, this system had disadvantages in practical use. Syntheses of such tripod-biomolecule conjugates were rather complicated, and therefore an alternative and more convenient approach was required in order to use the tripod molecule for immobilization of biomolecules on an AFM tip. In the present study, we have developed a new strategy using a Cu(I)-

catalyzed azide–alkyne cycloaddition reaction (CuAAC, commonly known as a "click" reaction) on the AFM-tip surface.[29,30] CuAAC is feasible under many bio-relevant conditions and provides the conjugation of biological molecules in sufficient yields.[31-33] It is also bio-orthogonal, water-compatible, and efficient under mild reaction conditions.[34-36] The recently developed strain-promoted copper free azide-alkyne cycloaddition is another attractive and bio-orthogonal method for conjugation of biomolecules.[37-39] Although this approach has been applied to many biological applications,[37-40] modifications of surfaces[41-43] including AFM tips,[44] it is reported to be much slower than CuAAC.[31,45]

In addition to the synthetic and biological applications of CuAAC, it has also been successfully employed for the modification of surfaces in the recent years.[46,47] However, there are only few reports in literature where this reaction was used for AFM-tip functionalization.[48,49] In this study, we will present a new, versatile and robust method of chemical functionalization of AFM-tips by biomolecules using an "*in situ click reaction*". Our present strategy includes the following steps (Fig. 1a): (1) immobilization of the tripod–acetylene **1** onto a gold-coated AFM tip surface (creation of "*pre-modified AFM tip*"), (2) attachment of a biomolecule (*e.g.* biotin) by the reaction of an azide group in a suitable linker attached to the biomolecule (*e.g.* N_3–PEG_{2000}–biotin **6** in Scheme 1) with the acetylene of the tip tripod *via* click chemistry (so-called *in situ* attachment of a biomolecule on the AFM tip surface: *on-tip-reaction*). We use biotin as a standard biomolecule and carry out force-spectroscopy experiments with a NeutrAvidin-coated substrate to test the strategy of "*in situ fishing*" of biomolecules by an AFM tip.

2. Experimental Section

2.1 Synthesis of tripod molecules

The tripod **1** with a terminal acetylene group (Fig. 1b), N_3–PEG_{2000}–biotin **6** and tripod–PEG_{2000}–biotin **2** (Scheme 1) were synthesized as previously reported[21] with slight modifications. Syntheses of tripod **1**, N_3–PEG_{2000}–biotin **6** and tripod–PEG_{2000}–biotin **2** are shown in Schemes S1, S2 (ESI) and 1.

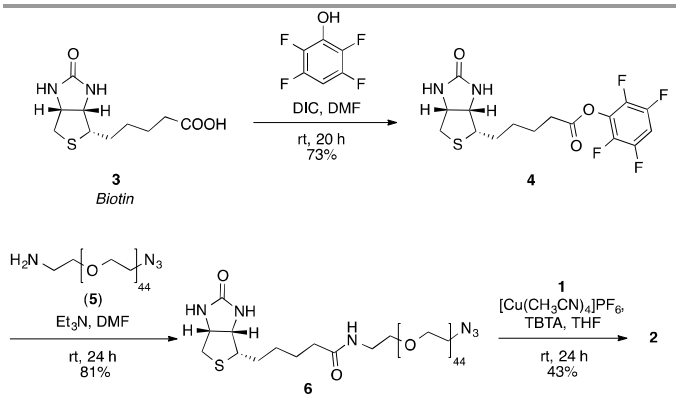

Scheme 1. Synthesis of PEGylated biotin **6** and molecular tip **2**.

2.2 Surface analyses of a flat gold surface after immobilization of tripod 1 and subsequent click reaction

Prior to the functionalization of a Au-coated AFM-tip, as a preliminary study, the flat gold surface was subjected to immobilization of the tripod and subsequent click reaction, and then was analysed by surface characterization methods. The outline of surface preparation is illustrated in Fig. 2.

Immobilization of tripod 1 on flat gold surface (*surfaces A* and *B*). An ultraflat gold surface was prepared by the template-stripping method, as described elsewhere.[50] First, 200 nm of Au was deposited on a freshly cleaned silicon wafer (Si-materials, Kaufering, Germany) by an evaporation method using a BalTec MED020 sputter coating unit (BalTec AG, Liechtenstein). The initial deposition rate during the evaporation was maintained below 0.05 nm/s for the first 10 nm, in order to control the roughness of the template-stripped surface. In the next step, the evaporated surface was glued onto a glass slide using an UV-curable glue (Norland Optical Adhesive 61, Norland Products, Cranbury, NJ, USA). In the last step, immediately before use, the silicon template was stripped away to reveal an ultraflat gold surface (Fig. 2, *surface A*).

The obtained Au surface was cleaned by a UV/ozone treatment for 1 hr using an UV/Ozone Procleaner™ Plus (BioForce Nanosciences). The gold substrate was then soaked in a filtered (0.45 µm CHROMAFIL® Xtra PTFE-45/25, Machery-Nagel GmbH & Co. KG, Düren, Germany) solution of tripod **1** (100 µM) in DMSO (UV spectroscopy grade, Fluka) for 13 hrs at room temperature. After washing thoroughly with DMSO, water, toluene and ethanol, the substrate was dried under a N_2 stream and subjected to the surface analyses below (Fig. 2, *surface B*).

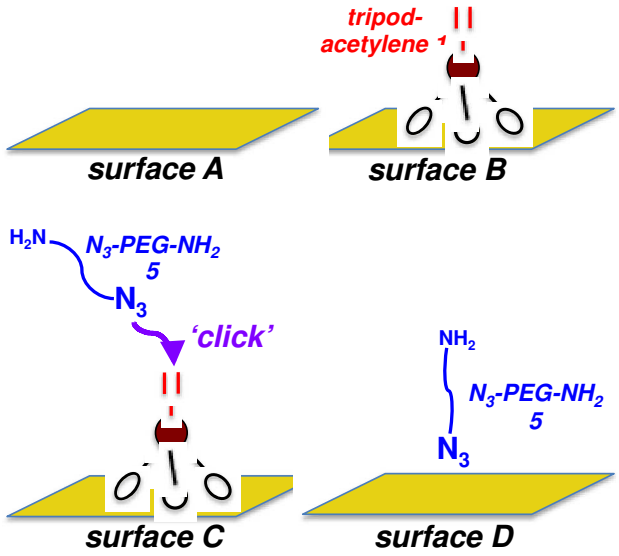

Fig. 2. Schematic illustration of surface modification of flat Au surface for the general surface characterizations; *surface A*: clean ultraflat Au surface, *surface B*: Au surface treated with tripod–acetylene **1**, *surface C*: Au surface with **1** treated under a click condition, *surface* D: Au surface without **1** treated under a click condition (control experiment).

Click reaction on flat Au surface (*surfaces C* and *D* (control)). The flat gold substrate modified by the tripod **1** (*surface B*) was soaked in a filtered solution of click reagents containing N_3–PEG_{2000}–NH_2 **5** (5.0 µmol), $[Cu(MeCN)_4]PF_6$ (25 µmol) and tris(benzyltriazolylmethyl)-amine (TBTA) (25 µmol) in 6 mL THF (HPLC grade, Sigma-Aldrich) at room temperature for 10 hrs. Subsequently, the substrate was thoroughly washed with THF, DMSO, water, toluene and ethanol. After drying under a N_2 stream, it was subjected to the surface analyses described below (Fig. 2, *surface C*). As a control experiment, a gold substrate, which was not treated with tripod **1**, was subjected to the identical click conditions as above. The substrate was subsequently washed thoroughly with DMSO, water, toluene and ethanol before subjected to the surface analyses below (Fig. 2, *surface D*).

Contact angle measurements. Static water contact angles were measured at three different points on the substrates at room temperature and ambient humidity with a contact-angle goniometer (Ramé Hart model 100, Ramé Hart Inc., Succasunna, NJ, USA). For these measurements, 3 µl of milliQ water were used to form a drop on the gold surface.

AFM imaging. AFM imaging was carried out using a Bruker Dimension Icon AFM (Bruker Co.) under ambient conditions in tapping mode using a silicon cantilever (AC 160, Olympus, Tokyo, Japan).

Polarization-modulation infrared reflection-absorption spectroscopy (PM-IRRAS). Polarization-modulation infrared reflection-absorption spectra (PM-IRRAS)[51] were recorded on a Bruker IFS 66v IR equipped with a PMA 37 polarization-modulation accessory (Bruker Co.). A KRS-5 wire-grid polarizer was placed at the entrance of the incoming beam from the external beam port of the spectrometer, and modulated by a ZnSe photoelastic modulator. The beam was reflected off the sample surface at an angle of 80° and detected with a liquid-nitrogen-cooled MCT detector. The maximum in polarization retardation was set at 3000 cm^{-1}, and the polarization was modulated with a frequency of 50 kHz. The sample compartment was continuously purged with dry air during the measurements. The spectral resolution was set to 4 cm^{-1} with a 2 mm aperture. The multiplexed interferograms were acquired from 1024 scans. The data was processed with OPUS software (Bruker Optics, Germany) and the baseline corrected with a polynomial function.

2.3 Quartz Crystal Microbalance (QCM) measurements

Quartz Crystal Microbalance (QCM) analysis was used to monitor the adsorption of tripod–acetylene **1** and subsequent click reaction with N_3–PEG_{2000}–NH_2 **5** on the flat gold surface. Measurements were carried out using a QCM-D (Q-sense AG, Gothenburg, Sweden) at 25 °C and analysed using Qsoft 401 software (Q-sense AG). A gold-coated QCM quartz crystal (Q-sense AG) was cleaned by sonication in ethanol and subsequently by plasma cleaning for 1 hr, and was mounted into the QCM cell. Pure DMSO was injected into the cell until a stable frequency baseline was obtained. A filtered solution of tripod **1** (100 µM in DMSO) was injected into the chamber. After 47 min, when the crystal was saturated by tripod adsorption, the chamber was rinsed by the injection of pure DMSO for 20 min. Later, it was flushed with pure THF for 45 min to obtain a baseline frequency for THF. A filtered click solution in THF (6 mL), which was the same as used above for the Au surface, containing N_3–PEG_{2000}–NH_2 **5** (5.0 µmol), $[Cu(MeCN)_4]PF_6$ (25 µmol) and TBTA (25 µmol), was injected into the cell using a glass syringe. After intermittent injection for 85 min, pure THF was again injected for 20 min to remove the unbound materials, followed by injection of pure DMSO for the next 50 min.

2.4 Gold-coated AFM tip functionalization

Gold-coated silicon nitride cantilevers (NPG, Veeco Instruments, Santa Barbara, CA, USA) were cleaned by UV/ozone treatment for 30 min and then soaked overnight in a filtered solution of tripod **1** (100 µM in DMSO) or a filtered solution of tripod–PEG_{2000}–biotin **2** (200 µM in DMSO) using a homemade teflon-coated cantilever holder. Subsequently, they were exhaustively washed with DMSO, water, toluene and ethanol. The tip modified by tripod **1** was soaked overnight at room temperature in a filtered solution of click reagents containing N_3–PEG_{2000}–biotin (**6**) (5.0 µmol), $Cu[(MeCN)_4]PF_6$ (25 µmol) and TBTA (25 µmol) in 6 mL THF. Subsequently, the cantilever was thoroughly washed with THF, DMSO, water, toluene and ethanol. The two cantilevers were dried under a N_2 stream and mounted on the cantilever holder for the AFM force-spectroscopy experiments.

2.5 Chemical force spectroscopy

Force measurements were carried out with a Molecular Force Probe (MFP-3D AFM, Asylum Research, Santa Barbara, CA, USA). The NeutrAvidin-coated agarose beads (immobilized NeutrAvidin Protein 29200, Pierce Biotechnology Inc., Rockford, IL, USA) were placed on a freshly cleaned glass slide and measurements were carried out in 20 mM HEPES buffer (pH 7.4). Force *vs* distance curves were taken with a scan rate of 0.12 Hz and a tip velocity of 500 nm/s over a z-piezo distance of 2 µm. The spring constants of the cantilevers were calibrated by the thermal-noise method prior to the modifications.[52]

3. Results and Discussion

Syntheses of tripods and their stability

The tripod molecule **1** containing a terminal acetylene moiety, a rigid adamantane core and three rigid phenyl acetylene legs with terminal disulfide moieties for a firm attachment *via* six Au–S bonds, was synthesized by a standard multistep organic synthesis and purified before use.[21] This tripod **1** was bench stable at room temperature for many days and can be stored at lower temperature for years. It was compatible with many solvents such as CH_2Cl_2, $CHCl_3$, THF, DMSO and water. The Pd-mediated Sonogashira coupling reaction and Cu-catalyzed click reaction were reliably performed for the modification of

the alkyne moiety in solution phase. It is expected to be stable on the gold surface for a long period due to its stable attachment through a total of six Au–S covalent bonds.

In situ click chemistry on the flat gold substrate

Prior to the modification and characterization of gold AFM tips of very small area, we used an ultraflat gold surface with a larger surface area to carry out a preliminary test of the surface reaction that could be better monitored by surface characterization methods such as contact angle, AFM imaging, PM-IRRAS and QCM. Immobilization of **1** on a Au surface through Au–S chemistry was carried out by a standard solution method. To further test the feasibility of an *in situ* click reaction on a gold surface, a commercially available polyethylene glycol-azide derivative **5** (N_3–PEG_{2000}–NH_2) was subjected to the reaction with the pre-attached tripod–acetylene on the gold substrate. The reaction was carried out in THF at room temperature, using $[Cu(MeCN)_4]PF_6$ as a Cu(I) source, which is stabler and more soluble in THF compared to CuI, that was used initially and caused the generation of insoluble precipitates, which interfered with subsequent surface analyses, such as AFM imaging.

Contact angle measurements

Static water-contact angle measurements were used to study the changes in the hydrophobicity of the substrates, to look for evidence of a successful surface-click reaction. For the tripod-molecule-functionalized Au substrate (*surface B*), the water contact angle was 123±1°. This large value of the contact angle, when compared to the initial, clean Au surface (*surface A*, 50±0°), indicates increased hydrophobicity of the surface due to the presence of organic moieties such as the adamantane core and phenylacetylene units of tripod **1**. After the click reaction with N_3–PEG_{2000}–NH_2 **5**, the water static contact angle of the surface changed to a value of 61±1° (*surface C*). This large decrease in the contact angle indicates the increase in the hydrophilicity of the surface and therefore, supports the presence of PEG moieties bound on the surface. In contrast, a control experiment on a Au surface without initial adsorption of tripod **1**, but treated under a click reaction condition (*surface D*), showed a static water contact angle of 53±0°, which was almost identical to that of the clean Au surface. This result clearly indicates that non-specific adsorption of N_3–PEG_{2000}–NH_2 **5** on the surface did not occur in the absence of tripod **1** on the Au, confirming the successful and specific *in situ* click reaction of a terminal alkyne of tripod **1** and an azide group of N_3–PEG_{2000}–NH_2 **5** on the Au surface.

AFM imaging

The Au surface was analysed by AFM imaging after the attachment of **1** (*surface B*), and compared to the initial ultraflat Au surface (*surface A*) (Figs. S1 and S2 in the ESI). The initial unfunctionalized Au surface showed a roughness of 0.36 nm (Fig. S1), whereas the surface treated with tripod **1** showed the rms roughness as 1.60 nm (Fig. S2). This higher roughness indicates that the stiffer tripod–acetylene **1** adsorbed on the gold surface.

The surface after the click reaction (*surface C*) was observed to be smoother with the rms roughness of 0.6 nm in comparison to the surface before the reaction (Fig. S3). This decrease of roughness compared to the surface before the reaction can be explained by the speculation that chemically attached flexible PEG moieties lie down under dry condition and cover the rough surface produced by the immobilized tripod molecule and thus lead to a smoother surface.

PM-IRRAS measurements

Infrared spectroscopy was used to support the evidence of tripod–acetylene **1** immobilization and subsequent *in situ* click reaction on Au surface. Two ultraflat Au substrates were treated for 2 hrs with a DMSO solution of tripod **1** as described above (*surface B*). After thorough washing with solvents, one of the Au substrates with **1** was soaked in the click solution of N_3–PEG_{2000}–NH_2 **5** (*surface C*). As a control experiment, one additional gold substrate, which was not treated with tripod **1**, was also soaked to the click solution of **5** (*surface D*). All the substrates were washed thoroughly with solvents and then dried under N_2 before being analysed by PM-IRRAS. The results are summarized in Fig. 3, in red line (*surface B*), blue line (*surface C*) and black line (*surface D*). It should be noted that a monolayer consisting of a low surface density of molecules can result in noisy IR spectra.

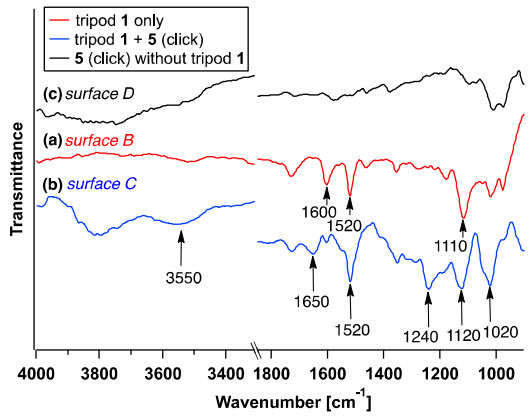

Fig. 3. Partial PM-IRRAS spectra of (a) gold substrates after tripod immobilization (red line), (b) subsequent click reaction with PEG azide **5** (blue line), and (c) a control experiment under click conditions on the bare gold surface in the absence of the tripod molecule (black line). A strong band at 1240 cm^{-1} corresponding to CH_2 bending of the PEG moiety and a broad band centred at 3550 cm^{-1} due to N-H stretching were observed after the click reaction with **5** (b) while these specific peaks were absent on the tripod-modified (a) and control surfaces (c). Full PM-IRRAS spectra of these substrates are shown in Fig. S4 in ESI.

For the gold surface with tripod **1** before click reaction (*surface B,* Fig. 3a, red line), two bands at 1600 and 1520 cm^{-1} corresponding to the aromatic rings were observed. These bands were also observed in bulk FT-IR measurements of tripod **1** (Fig. S5). Another strong band at 1110 cm^{-1} was also observed. After subjecting to the click reaction (*surface C,* Fig. 3b, blue line) with N_3–PEG_{2000}–NH_2 **5**, a band at 1240 cm^{-1} due

to CH_2 bending of the PEG moiety and a broad band centred at 3550 cm^{-1} arising from N–H stretch of terminal amine group were observed. In addition, the peak corresponding to the C–O–C stretch in the PEG moiety was observed at 1120 cm^{-1}. In contrast, the control surface (*surface D*) did not show any significant band (Fig. 3c, back line). These results clearly indicate the chemical attachment of N_3–PEG_{2000}–NH_2 **5** with tripod–acetylene *via* the click reaction and not through physical adsorption onto the gold surface.

QCM measurements

QCM is a very efficient and sensitive technique for studying the real-time adsorption of molecules on the surface.[53,54] To monitor the time-dependent adsorption of tripod molecules on the gold surface and to study the efficiency of the *in situ* click reaction, QCM analyses were undertaken using QCM-D (Q-sense AG). The results are shown in Fig. 4.

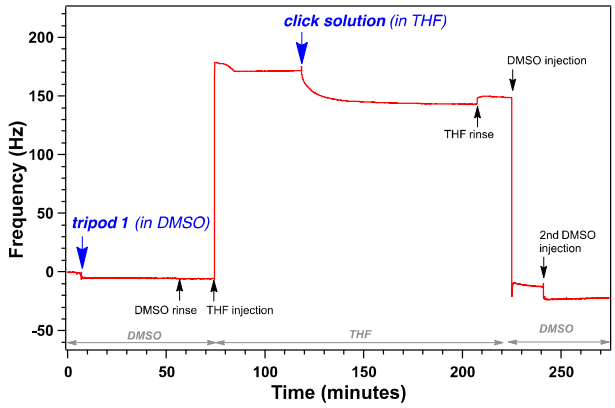

Fig. 4. QCM curves upon treatment with tripod **1** and subsequent click reaction with PEG azide **5**. The crystal was excited to oscillate at its resonant frequency, and changes in the frequency were monitored upon injection of DMSO, tripod **1**, THF and click solution [**5**, Cu(I) and TBTA] in THF for the 1st, 3rd, 5th, 7th, 9th and 11th overtones. The data shown here is the frequency *vs* time scaled by its overtone order (11th). From the Sauerbrey equation, the total masses adsorbed upon treatment with tripod and subsequent click reaction were calculated as 100.8 ng/cm^2 and 389.4 ng/cm^2 respectively.

First, pure DMSO was injected into the cell containing the gold-coated quartz crystal, to obtain a stable baseline in oscillation frequency. Following this, a filtered solution of tripod **1** in DMSO (100 µM) was injected and a sharp decrease in the oscillation frequency was observed. The frequency did not change further with time, implying the very fast and saturated adsorption of tripod **1** on gold surface. Also, when pure DMSO was re-injected to remove the unbound molecules, no further change was observed, indicating the covalent and stable attachment of tripod **1** *via* Au–S bond formation. To further examine the *in situ* click reaction on the modified gold-coated quartz crystal, the same conditions as applied for *in situ* click reaction for the gold surface modification were used. For this, the solvent was switched from DMSO to THF (HPLC grade, Sigma-Aldrich) and a large shift (increase) in the frequency was seen, possibly due to a lower density of THF (0.889 g/cm^3) compared to DMSO (1.10 g/cm^3).

Next, a filtered click solution, as used above (5 µmol of azide **5**, 25 µmol of each $[Cu(MeCN)_4]PF_6$ and TBTA in 6 mL THF), was injected, and gradual lowering of the frequency was recorded. The frequency nearly remained constant after about 1.5 hrs, indicating no further adsorption of molecules on the crystal. Upon washing the crystal with excess THF to remove the unbound materials, the frequency only slightly changed, which confirms covalent attachment of **5** and thus the successful click reaction on the quartz crystal. As the baseline of THF and DMSO are different, to compare the shift in the frequency after click reaction to that after tripod **1** adsorption, pure DMSO was again injected. The frequency was lowered significantly and to a value lower than that after tripod adsorption. When DMSO was again injected, the value of the oscillation frequency decreased further, but it did not change after a third injection, and remained constant afterwards. This could be due to some THF being left on the surface after the first injection and subsequently being completely washed upon the second injection of excess DMSO. From the frequency shift (Δf), the adsorbed mass per unit area (Δm) was obtained by using the following Sauerbrey equation.

$$\Delta m = -C \times \Delta f/n$$

C is the sensitivity constant of the quartz crystal and n is the overtone number. From the Sauerbrey equation, the total masses adsorbed upon treatment with tripod and subsequent click solution were measured to be 100.8 ng/cm^2 and 389.4 ng/cm^2 respectively. The surface density of the tripod molecule calculated from this mass was ~10^{13} molecules/cm^2, which is approximately the same as that obtained for the fully covered gold surface by the tripod molecule (calculated from the surface area of the single tripod molecule). Similarly, the surface density of the PEG-azide **5** attached *via* a click reaction was also calculated to be ~10^{13} molecules/cm^2 indicating that essentially all the tripod molecules on the surface reacted with **5** under the applied click conditions.

In situ click chemistry on AFM tip and force measurements

Based on the promising preliminary results of the surface click reaction on the ultraflat gold surface above, which were further confirmed by the QCM experiments, a reaction on the gold-coated AFM tip was carried out. A commercially available gold-coated AFM tip was used for the immobilization of tripod **1** in a similar way to that used for the ultraflat gold surface. The AFM tip with tripod **1** was subsequently subjected to a click reaction with N_3–PEG_{2000}–biotin **6**. As a positive control experiment, tripod–PEG_{2000}–biotin **2** was also used for the functionalization of Au-AFM tip surface.

A commercially available, gold-coated cantilever was calibrated, cleaned by UV/ozone treatment, mounted on a homemade teflon holder and soaked overnight in a filtered solution of tripod **1** in DMSO (100 µM). The cantilever was thoroughly washed with DMSO, water, toluene and ethanol and subsequently soaked in a filtered click solution containing 5 µmol of **6**, 25 µmol (5 equiv to **6**) of each $[Cu(MeCN)_4]PF_6$ and

TBTA in 6 mL of THF. After 15 hrs, the cantilever was washed with THF, water, toluene and ethanol and subjected to force measurements with NeutrAvidin.

NeutrAvidin-coated agarose beads were deposited on a piece of clean glass slide and used as a substrate. Force–distance measurements were carried out in HEPES buffer. AFM tip was positioned on the top of the bead to avoid any non-specific interactions with glass slide. Nearly 74% of the measurements showed a detectable rupture force, and in some cases, more than one rupture force per measurement was observed during the retraction of the tip. The average number of detectable forces per measurement was 1.7. The length of tripod–PEG_{2000}–biotin **2** in its extended form was estimated to be 19 nm using Spartan 08 (Wavefunction, Inc., Irvine, CA, USA). Assuming that the molecular tip obtained by the *in situ* click reaction cannot extend more than approximately 20 nm, the rupture forces between 10-20 nm distance were collected and subjected to histogram analysis as shown in Fig. 5a. The rupture forces were mainly distributed in the range of 50-275 pN, with a significant number between 100-125 pN. The centre of the force distribution obtained from a Gaussian fit of the histogram was found to be 104±5 pN. To confirm that the obtained force distribution curve corresponds to the interactions between biotin on the tip and NeutrAvidin on the substrate, the same measurements were carried out in the presence of an excess amount of biotin in HEPES (0.22 mg/mL).

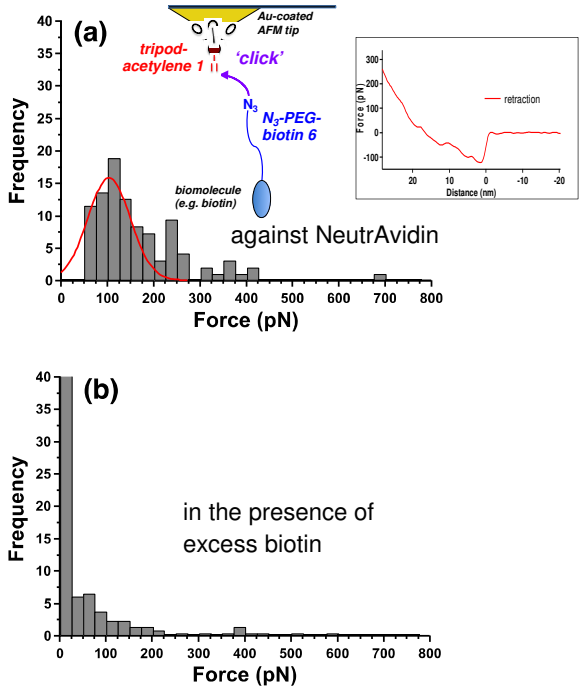

Fig. 5. (a) Histogram of biotin–NeutrAvidin rupture forces using an AFM tip modified by surface click chemistry (inset: a typical force–distance curve). The centre of the force distribution from a Gaussian fit is 104±5 pN. (b) In the presence of excess biotin in the measurement solution. The majority of forces observed in the above case were diminished. Caluculated loading rate was 4.75 x 10^4 pN/s.

As shown in Fig. 5b, most of the rupture forces in 50-275 pN regions were significantly diminished and forces of lower magnitude, which presumably correspond to the nonspecific interactions between the tip and surface, were observed. Additionally, only 26% of the total measurements showed any detectable rupture force, including those of lower magnitude. From this experiment, it is clear that the forces obtained with AFM tip modified by *in situ* click chemistry were as a result of the specific interaction of ligand (biotin on tip) and the receptor (NeutrAvidin).

As a standard experiment, the tripod **2** (tripod–PEG_{2000}–biotin) was used for gold AFM tip modification and force spectroscopy experiments. A calibrated AFM tip was cleaned and then soaked overnight in a filtered DMSO solution (200 µM) of **2**. After thorough washing, it was used for the force–distance measurements with NeutrAvidin in HEPES buffer under the conditions used in above case. As a result, 90% of the measurements showed at least one detectable rupture force and the average number of forces per measurement were calculated to 2.2. The histogram of rupture forces with distance between 10-20 nm is shown in Fig. 6a. Similar to the above experiment where the ligand was attached by *in situ* click modification, the major forces were observed in the range of 50-350 pN with a centre of the distribution at 103±7 pN (Fig. 6a). The addition of excess biotin to the NeutrAvidin substrate in HEPES resulted in the diminishing of these forces and the recording of lower-magnitude non-specific forces (Fig. 6b).[21]

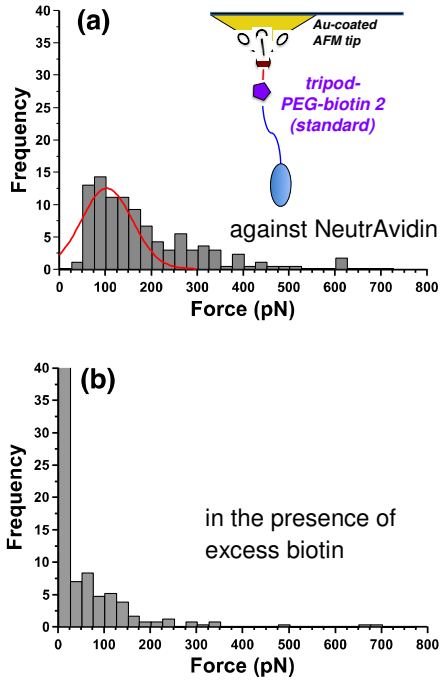

Fig. 6. Histogram of biotin–NeutrAvidin rupture forces (a) using an AFM tip modified with **2**. The centre of the force distribution from a Gaussian fit is 103±7 pN. (b) In the presence of excess biotin in the measurement solution. Caluculated loading rate was 5.8 x 10^4 pN/s.

Two additional control experiments were also carried out where the rupture forces were measured using the AFM tips functionalized with; (I) tripod **1** (without ligand) against NeutrAvidin-coated beads and, (II) molecule **2** against a glass substrate (without receptor) in buffer. The histograms of the rupture forces are shown in Fig. 7. As shown in Fig. 7a, the tip functionalized with tripod **1** (control experiment I) showed no significant rupture force distribution against NeutrAvidin as a substrate and only non-specific forces of a lower magnitude were observed. In control experiment II, where the interactions of an AFM tip functionalized with molecule **2** were studied with the glass substrate, although many rupture forces occurred over a wide range of magnitudes (Fig. 7b), there was no specific distribution corresponding to the specific interactions. These results also confirm that the distribution peaks observed in Figs. 5a and 6a are corresponding to the specific biotin–NeutrAvidin rupture forces.

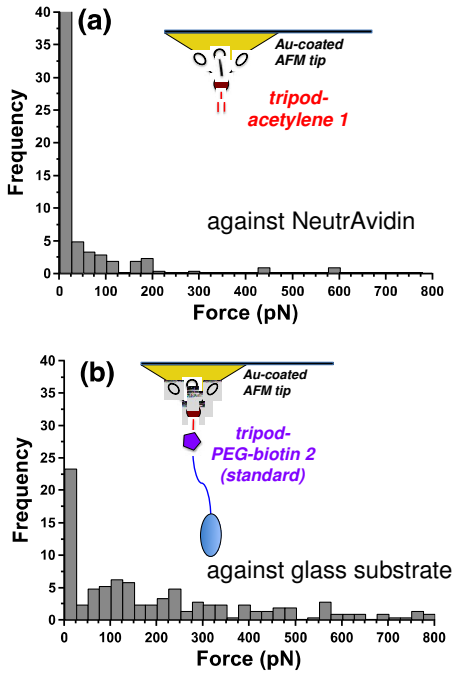

Fig. 7. Histogram of forces obtained from force–distance measurements: (a) using a tip functionalized with tripod **1** against NeutrAvidin in HEPES; (b) using a tip functionalized with **2** against a glass substrate in HEPES buffer. The larger forces (800-1600 pN) were also observed in the measurements of (b) but without specific distribution.

Conclusions

A versatile and general method for the immobilization of biomolecules on gold-coated AFM tip was developed by using an *in situ* click reaction on a tip with a pre-attached tripod–acetylene **1**. The initial immobilization of tripod **1** on the gold and the subsequent click reaction of the acetylene moiety with N_3–PEG_{2000}–NH_2 **5** were confirmed by surface analysis methods, such as AFM imaging, PM-IRRAS and static water contact angle measurements using a flat gold surface. The real-time attachment of tripod molecule and subsequent connection of PEG azide **5** on the gold surface was also studied by QCM measurements. A gold AFM tip was subjected to the same treatment (addition of tripod–acetylene **1** and subsequent *in situ* click reaction with biotin–PEG_{2000}–N_3 **6**), which was followed by force–distance measurements using NeutrAvidin. A significant distribution peak corresponding to the biotin-NeutrAvidin unbinding force was observed, which was in a good agreement with the result obtained when a tripod–PEG_{2000}–biotin **2** immobilized tip was used. The centre value of the distribution curve in both cases was approximately 104 pN. These forces disappeared when the measurements were carried out in the presence of excess biotin in HEPES buffer. These results reveal an efficient functionalization of the AFM tip by the *in situ* click protocol. This approach provides an effective and convenient tool for the immobilization of various biomolecules on the AFM tip using a stable, wider tripodal scaffold.

Acknowledgements

The authors thank Dr. Deepak Kumar and Dr. Qingling Xu from ETH-Zürich for their contributions to obtaining the preliminary results. This research was supported in part by Swiss National Foundation (200021-140451, 200021-156097, YY).

Notes and references

[a]*Laboratorium für Organische Chemie, ETH-Zürich, Vladimir-Prelog-Weg 3, CH-8093 Zürich, Switzerland*

[b]*Laboratory for Surface Science and Technology, Department of Materials, ETH-Zürich, Vladimir-Prelog-Weg 5, CH-8093 Zürich, Switzerland*

† Electronic Supplementary Information (ESI) available: Experimental details with synthesis and characterization of compounds. Procedures for modifications of Au surfaces and AFM tips. AFM images and full PM-IRRAS spectra of modified surfaces. Detailed procedure for QCM measurement. A table showing ligand-receptor interaction probability. NMR, IR and MS charts. See DOI: 10.1039/b000000x/

‡ R.K. and S.N.R. contributed equally.

References

1. C. D. Frisbie, L. F. Rozsnyai, A. Noy, M. S. Wrighton and C. M. Lieber, *Science*, 1994, **265**, 2071–2074.
2. A. Noy, C. D. Frisbie, L. F. Rozsnyai, M. S. Wrighton and C. M. Lieber, *J. Am. Chem. Soc.*, 1995, **117**, 7943–7951.
3. D. V. Vezenov, A. Noy, L. F. Rozsnyai and C. M. Lieber, *J. Am. Chem. Soc.*, 1997, **119**, 2006–2015.
4. C. A. Bippes and D. J. Muller, *Rep. Prog. Phys.*, 2011, **74**, 086601.
5. P. E. Marszalek and Y. F. Dufrêne, *Chem. Soc. Rev.*, 2012, **41**, 3523–3534.
6. M. Rief, M. Gautel, F. Oesterhelt, J. M. Fernandez and H. E. Gaub, *Science*, 1997, **276**, 1109–1112.
7. S. S. Wong, E. Joselevich, A. T. Woolley, C. L. Cheung and C. M. Lieber, *Nature*, 1998, **394**, 52–55.
8. C. Yuan, A. Chen, P. Kolb and V. T. Moy, *Biochem*istry, 2000, **39**, 10219–10223.

9. Y. Shan, Z. Wang, X. Hao, X. Shang, M. Cai, J. Jiang, X. Fang, H. Wang and Z. Tang, *Anal. Methods*, 2010, **2**, 805–808.
10. J. G. Jiang, X. Hao, M. Cai, Y. Shan, X. Shang, Z. Tang and H. Wang, *Nano Lett.*, 2009, **9**, 4489–4493.
11. B. D. Sattin, A. E. Pelling and M. C. Goh, *Nucleic Acids Res.*, 2004, **32,** 4876–4883.
12. A. Noy, D. V. Vezenov, J. F. Kayyem, T. J. Meade and C. M. Lieber, *Chem. Biol.*, 1997, **4**, 519–527.
13. T. Strunz, K. Oroszlan, R. Schäfer and H. J. Güntherodt, *Proc. Natl. Acad. Sci. U.S.A.*, 1999, **96**, 11277–11282.
14. D. J. Müller and A. Engel, *Nat. Protoc.,* 2007, **2**, 2191–2197.
15. R. Barattin and N. Voyer, *Chem. Commun.*, 2008, 1513–1532.
16. T. Ito, I. Grabowska and S. Ibrahim, *TrAC, Trends Anal. Chem*., 2010, **29**, 225–233.
17. H. X. He, W. Huang, H. Zhang, Q. G. Li, S. F. Y. Li and Z. F. Liu, *Langmuir*, 2000, **16**, 517–521.
18. P. Hinterdorfer and Y. F. Dufrêne, *Nat. Methods*, 2006, **3**, 347–355.
19. Q. Li, A. V. Rukavishnikov, P. A. Petukhov, T. O. Zaikova and J. F. W. Keana, *Org. Lett.*, 2002, **4**, 3631–3634.
20. Q. Li, A. V. Rukavishnikov, P. A. Petukhov, T. O. Zaikova, C. Jin and J. F. W. Keana, *J. Org. Chem.*, 2003, **68**, 3631–3634.
21. M. E. Drew, A. Chworos, E. Oroudjev, H. Hansma and Y. Yamakoshi, *Langmuir*, 2010, **26**, 7117–7125.
22. Y. Yao and J. M. Tour, *J. Org. Chem.*, 1999, **64**, 1968–1971.
23. X. Deng and C. Cai, *Tetrahedron Lett.*, 2003, **44**, 815–817.
24. S. Zarwell and K. Rück-Braun, *Tetrahedron Lett.*, 2008, **49**, 4020–4025.
25. D. Takamatsu, Y. Yamakoshi and K. Fukui, *J. Phys. Chem. B*, 2006, **110**, 1968–1970.
26. D. Takamatsu, K. Fukui, S. Aroua and Y. Yamakoshi, *Org. Biomol. Chem.*, 2010, **8**, 3655–3664.
27. B. H. Kim, N. Y. Palermo, S. Lovas, T. Zaikova, J. F. W. Keana and Y. L. Lyubchenko, *Biochemistry*, 2011, **50**, 5154–5162.
28. E. L. Florin, V. T. Moy and H. E. Gaub, *Science*, 1994, **264**, 415–417.
29. H. C. Kolb, M. G. Finn and K. B. Sharpless, *Angew. Chem., Int. Ed.*, 2001, **40**, 2004–2021.
30. M. V. Gil, M. J. Arévalo and Ó. López, *Synthesis*, 2007, 1589–1620.
31. M. Yang, A. S. Jalloh, W. Wei, J. Zhao, P. Wu and P. R. Chen, *Nat. Commun.*, 2014, **5**, 4981-4990.
32. D. Soriano del Amo, W. Wang, H. Jiang, C. Besanceney, A. C. Yan, M. Levy, Y. Liu, F. L. Marlow and P. Wu*, J. Am. Chem. Soc*. 2010, **132**, 16893–16899.
33. C. Besanceney-Webler, H. Jiang, T. Zheng, L. Feng, D. Soriano del Amo, W. Wang, L. M. Klivansky, F. L. Marlow, Y. Liu and P. Wu, *Angew. Chem., Int. Ed*., 2011, **50**, 8051–8056.
34. C. Shao, G. Cheng, D. Su, J. Xu, X. Wang and Y. Hu, *Adv. Synth. Catal.* 2010, **352**, 1587–1592.
35. K. Wang, X. Bi, S. Xing, P. Liao, Z. Fang, X. Meng, Q. Zhang, Q. Liu and Y. Ji, *Green Chem*., 2011, **13**, 562–565.
36. S. Özçubukçu, E. Ozkal, C. Jimeno and M. A. Pericàs, *Org. Lett.*, 2009, **11**, 4680-4683.
37. J. M. Baskin, J. A. Prescher, S. T. Laughlin, N. J. Agard, P. V. Chang, I. A. Miller, A. Lo, J. A. Codelli and C. R. Bertozzi, *Proc. Natl. Acad. Sci. U. S. A.*, 2007, **104**, 16793–16797.
38. J. C. Jewett, E. M. Sletten and C. R. Bertozzi, *J. Am. Chem. Soc*., 2010, **132**, 3688–3690.
39. X. Ning, J. Guo, M. Wolfert and G.-J. Boons, *Angew. Chem., Int. Ed.,* 2008, **47**, 2253–2255.
40. J. C. Jewett and C. R. Bertozzi, *Chem. Soc. Rev*., 2010, **39**, 1272–1279.
41. R. K. Manova, S. P. Pujari, Carel A. G. M. Weijers, H. Zuilhof and Teris A. van Beek, *Langmuir*, 2012, **28**, 8651–8663.
42. A. Kuzmin, A. Poloukhtine, M. A. Wolfert and V. V. Popik, *Bioconjugate Chem*., 2010, **21**, 2076–2085.
43. S. V. Orski, A. A. Poloukhtine, S. Arumugam, L. Mao, V. V. Popik and J. Locklin, *J. Am. Chem. Soc*., 2010, **132**, 11024–11026.
44. S. Senapati, S. Manna, S. Lindsay and P. Zhang, *Langmuir*, 2013, **29**, 14622–14630.
45. S. I. Presolski, V. Hong, S. H. Cho and M.G. Finn, *J. Am. Chem. Soc.*, 2010, **132**, 14570–14576.
46. H. Nandivada, X. Jiang and J. Lahann, *Adv. Mater*., 2007, **19**, 2197–2208.
47. J. E. Moses and A. D. Moorhouse, *Chem. Soc. Rev.*, 2007, **36**, 1249–1262.
48. G. Chen, X. Ning, B. Park, G. J. Boons and B. Xu, *Langmuir*, 2009, **25**, 2860–2864.
49. F. Long, B. Cao, A. Khanal, S. Fang and R. Shahbazian-Yassar, *Beilstein J. Nanotechnol*. 2014, **5**, 2122–2128.
50. M. Hegner, P. Wagner and G. Semenza, *Surf. Sci*., 1993, **291**, 39–46.
51. M. A. Ramin, G. L. Bourdon, N. Daugey, B. Bennetau, L. Vellutini and T. Buffeteau, *Langmuir,* 2011, **27**, 6076–6084.
52. H. J. Butt and M. Jaschke, *Nanotechnology*, 1995, **6**, 1–7.
53. K. A. Marx, *Biomacromolecules*, 2003, **4**, 1099–1120.
54. S. K. Vashist and P. Vashist, *J. Sens.*, 2011, **2011**, 571405.

